Supporting information for: Structural Properties of Double-Walled Carbon Nanotubes Driven by Mechanical Interlayer Coupling

Ahmed Ghedjatti,[†] Yann Magnin,[‡] Frédéric Fossard,[†] Guillaume Wang,[¶] Hakim Amara,[*,†] Emmanuel Flahaut,[§] Jean-Sébastien Lauret,[‖] and Annick Loiseau[*,†]

[†]*Laboratoire d'Etude des Microstructures, ONERA-CNRS, BP 72, 92322 Châtillon Cedex, France*

[‡]*Aix-Marseille University and CNRS, CINaM UMR 7325, 13288 Marseille, France*

[¶]*Laboratoire Matériaux et Phénomènes Quantiques, CNRS-Université Paris 7, 10 rue Alice Domon et Léonie Duquet, 75205 Paris Cedex 13, France*

[§]*Centre Inter-universitaire de Recherche et d'Ingénierie des Matériaux (CIRIMAT), CNRS UMR 5085, Université Paul-Sabatier, 31062 Toulouse, France*

[‖]*Laboratoire Aimé Cotton, CNRS, Univ. Paris-Sud, ENS Cachan, Université Paris-Saclay, 91405 Orsay Cedex, France*

E-mail: hakim.amara@onera.fr; annick.loiseau@onera.fr

The DWNT samples under study

In Figure S1 we report the TEM analysis of our samples in term of population and diameter of tubes.

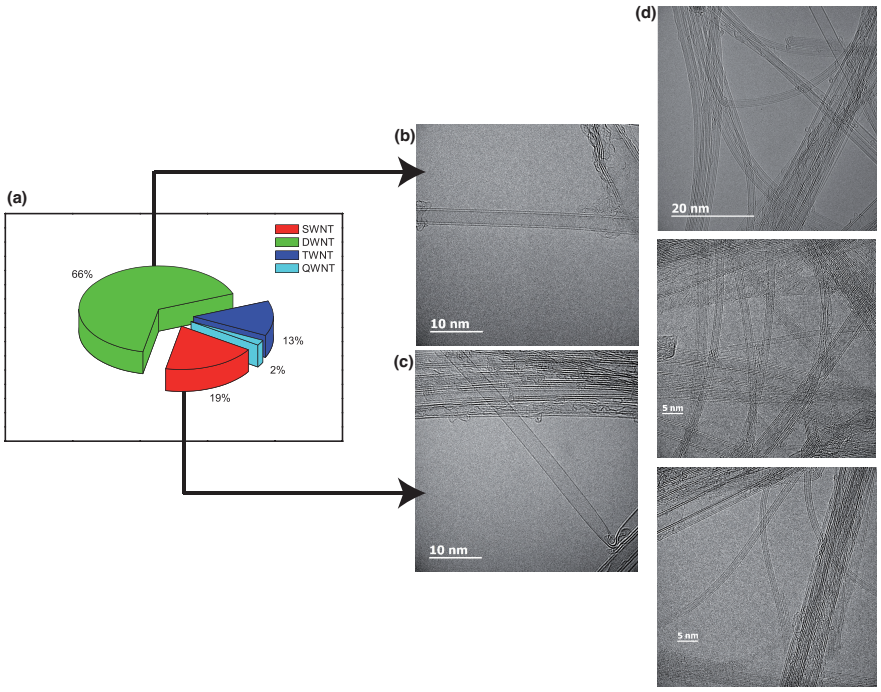

Figure S1: (a) Population of different kinds of tubes. HRTEM images of (b) DWNT, (c) SWNT and (d) raw samples we have analyzed where tubes are most often entangled.

Determination of tube diameters from TEM measurements

With the help of projected potential and simulation images, the two diameters of the constituent tubes in a DWNT are measured. A simple measurement of the distance between dark lines pairs, corresponding to the tube walls, exhibits a systematic and substantial deviation from the correct D, even for a SWNT, due to the unavoidable Fresnel fringes arising at the edges of the nanotubes.[S10,S11] In case of a DWNT, it is more complicated to measure the two diameters of the constituent tubes in a DWNT because of the more intense interference of Fresnel fringes between two adjacent tube walls. To get rid of such artefact, diameters have to be measured at the inversion point in the fringe profile. This can be done with the help of projected potential and simulation images and leads to precise D with an error $\sim$0.05 nm (see Figure S2 of the supporting information). Using the approach presented in Figure S2, we can obtain an error $\sim$0.05 nm whatever the atomic resolution of the TEM we use.

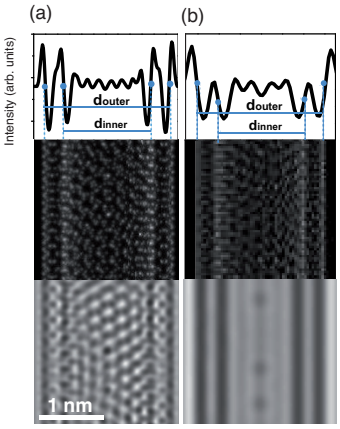

Figure S2: From bottom to top : simulated TEM image, projected potential image and profile of the equator line corresponding to the simulated TEM image. (a) New generation aberration-corrected microscope, the JEM-ARM-200F with a spatial resolution of 80 *pm* (b) Conventional microscope, the Philips CM-20 with a spatial resolution of 270 *pm*.

Various examples of DWNT structure determination

In Figure S3 and S4, various examples are presented showing the procedure to determine unambiguously DWNT structures.

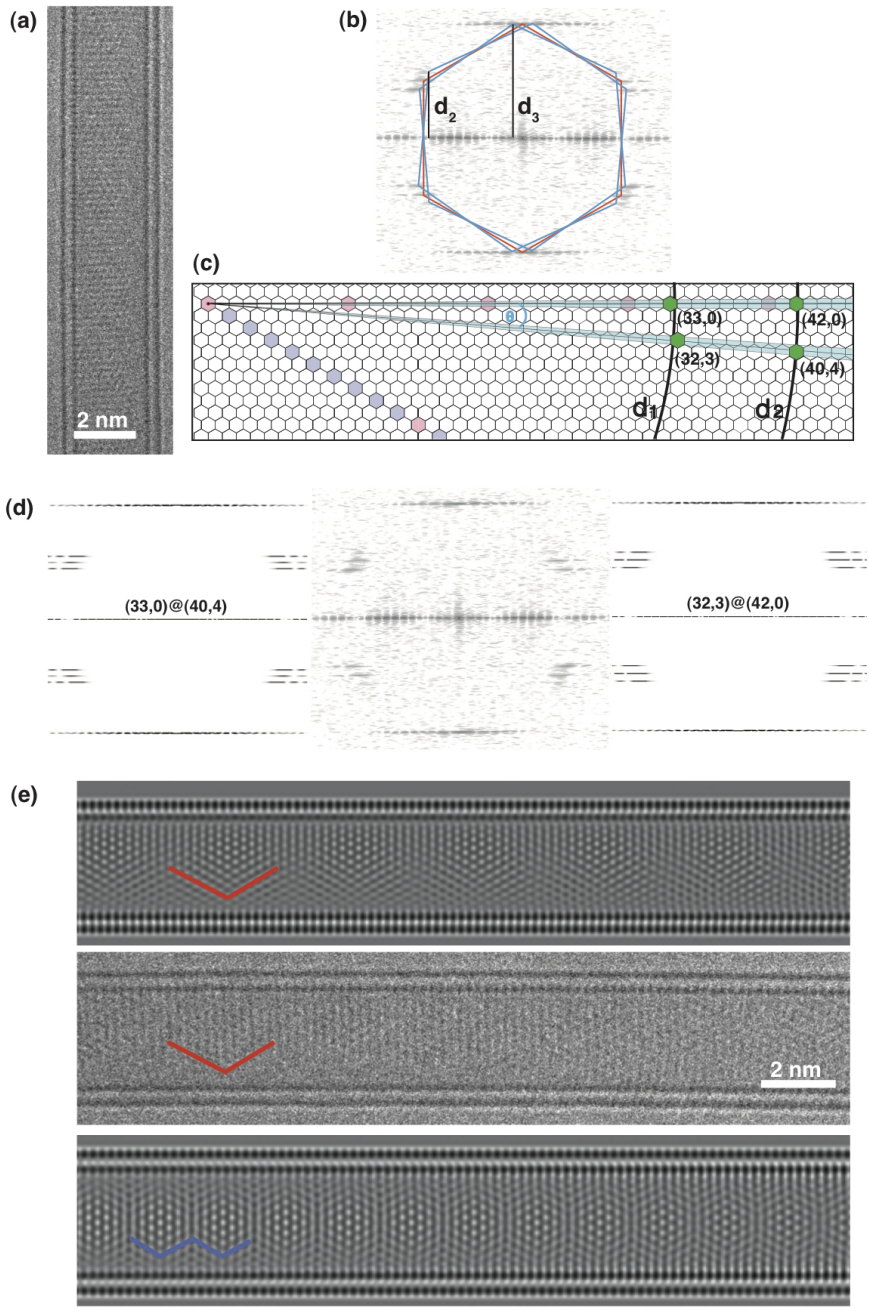

Figure S3: Determination of a (32,3)@(42,0) DWNT ($\Delta\theta = 4.43°$).(a) HR-TEM images of a DWNT and (b) its corresponding FFT. (c) Distribution of possible chiral indices after the analysis of the layer-lines. This lead to 2 configurations colored in green : (33,0)@(40,4) and (32,3)@(42,0). (d) Comparison of FFT from HR-TEM image and simulated results for previous solutions : no solution can be ruled out because differences are not significant. (d) Comparison of HR-TEM image and simulated images for deciding between the last configurations. Analysis of Moiré patterns, more precisely their sizes, enables to conclude that the investigated tube corresponds to (32,3)@(42,0) DWNT.

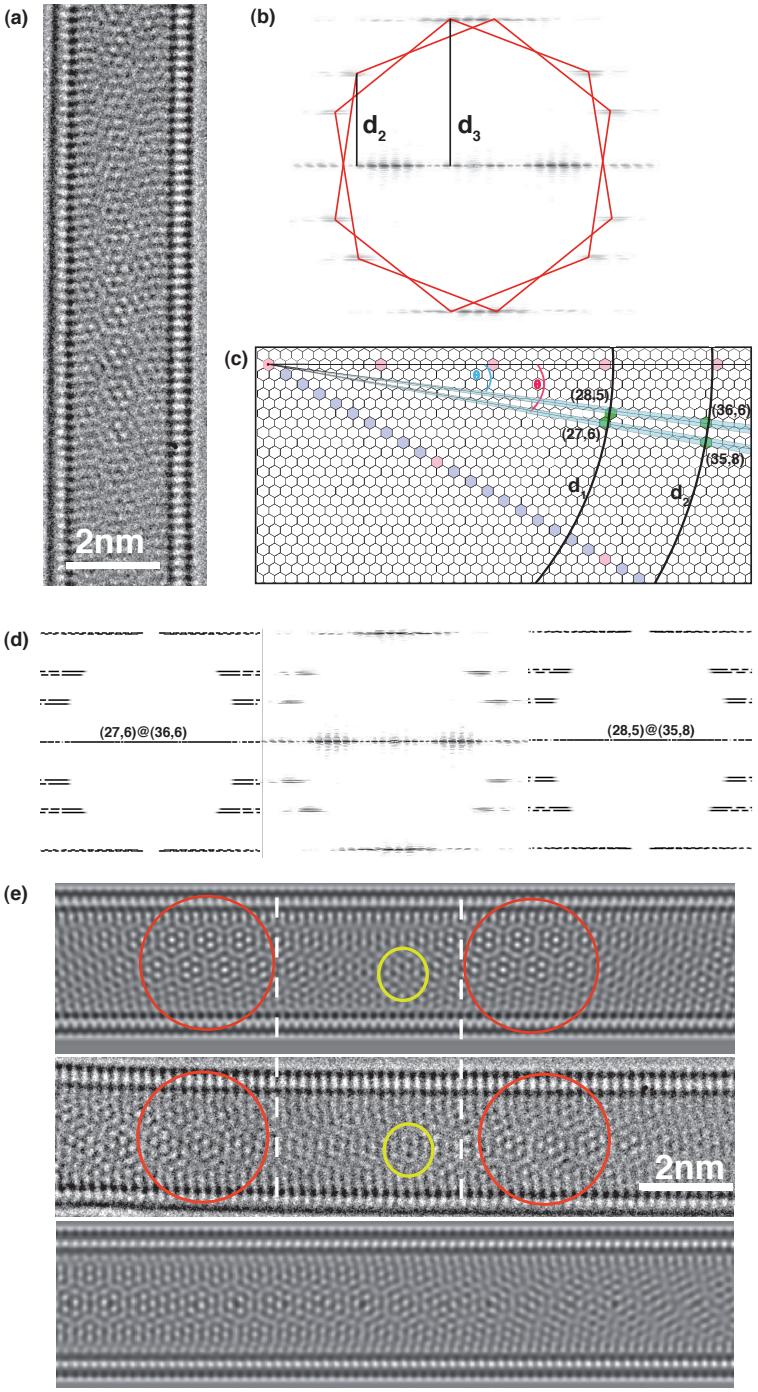

Figure S4: Determination of a (28,5)@(35,8) DWNT ($\Delta\theta \sim 2.0°$). (a) HR-TEM images of a DWNT and (b) its corresponding Fourier transform. (c) Distribution of possible chiral indices after the analysis of the layer-lines. This lead to 2 configurations colored in green : (28,5)@(35,8) and (27,6)@(37,6). (d) Comparison of Fourier transform from HR-TEM image and simulated results for previous solutions : no solution can be ruled out because differences are not significant. (d) Comparison of HR-TEM image and simulated images for deciding between the last configurations. Analysis of Moiré patterns enables to conclude that the investigated tube corresponds to (28,5)@(35,8) DWCNT.

Distribution of structural parameters

In Figure S5, we present the distribution of different structural parameters where it is clear that no correlation can be proposed.

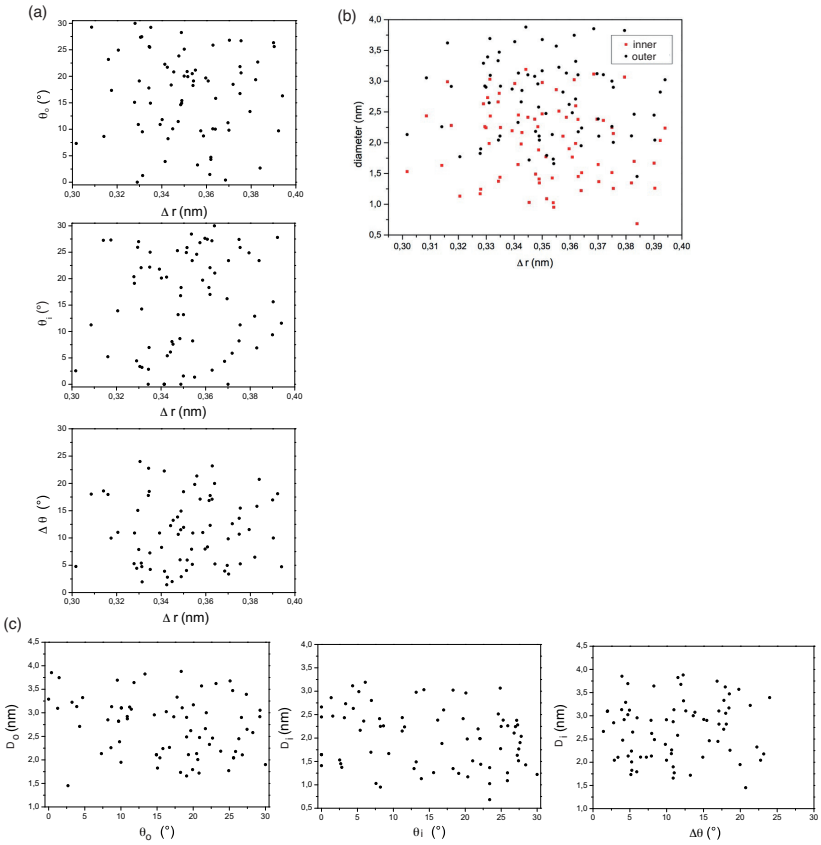

Figure S5: Distribution of structural parameters (Δr, θ_{in}, θ_{out} and $\Delta\theta$) of ~ 70 DWNTs. (a) Helicities as a function of Δr. (b) Diameter as a function of Δr. (c) diameter as a function of helicities.

Analysis of data from the literature

In Figure S6, we analyse the relationship between the helicities of outer tubes θ_o and $\Delta\theta$ from data found in the literature. Once again, forbidden configurations in grey areas ($\Delta\theta = 0°$ and $\Delta\theta > 25°$) have been found and a majority of DWNTs is depicted in a red square (both helicities are near armchair and $\Delta\theta < 15°$).

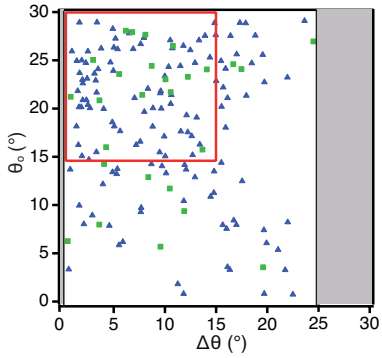

Figure S6: Statistical analysis of DWNT helicities extracted from different experiments using different synthesis techniques : arc discharge (green squares from Ref.[S12]) and CVD (blue triangles from Ref.[S13]).

Analysis of observed and non observed configurations

In Figure S7, analysis in term of local energies and C-C first neighbors intertube distances are presented for the observed (11,10)@(20,11) DWNT and non observed (8,8)@(13,13) DWNT.

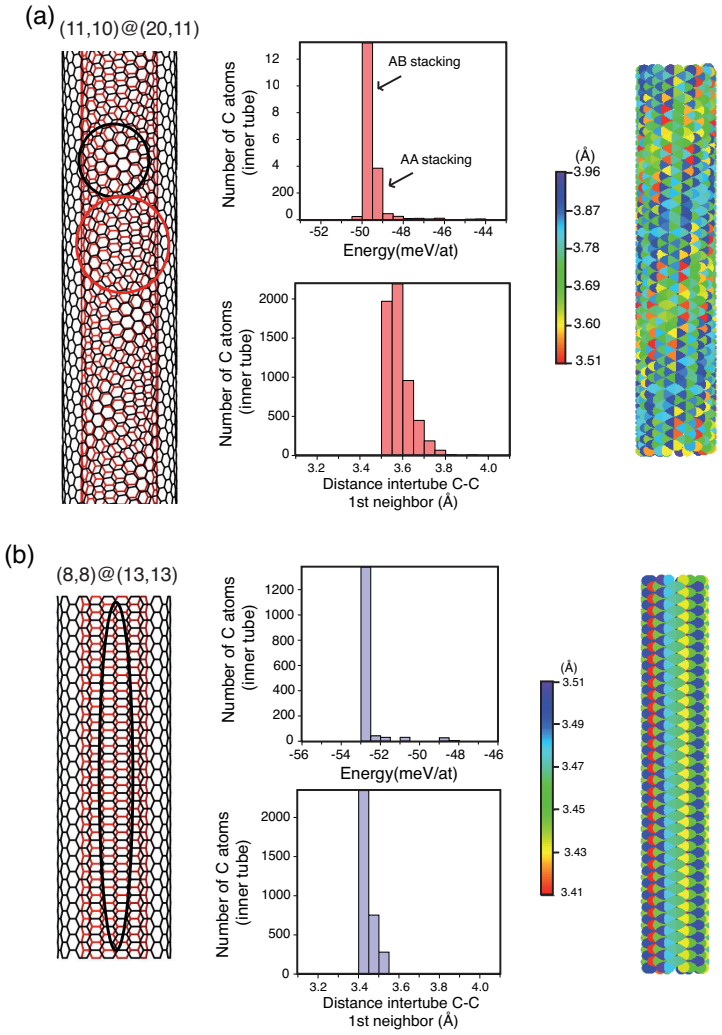

Figure S7: Analysis of local energies in form of histograms plot (middle). Different stackings (AA or AB) are highlighted by circles (left) and analysis of the C-C first neighbors intertube distances in form of histogram plots (middle) and spatial distribution along the tube (right). (a) (11,10)@(20,11) DWNT ($\Delta\theta = 20.48°$) and (b) (8,8)@(13,13) DWNT ($\Delta\theta = 0°$).

References

(S1) Flahaut, E.; Peigney, A.; Laurent, C.; Rousset, A. Synthesis of Single-Walled Carbon Nanotube-Co-MgO Composite Powders and Extraction of the Nanotubes. *J. Mater. Chem.* **2000**, *10*, 249-252.

(S2) Flahaut, E.; Bacsa, R.; Peigney, A.; Laurent, C. Gram-scale CCVD Synthesis of Double-Walled Carbon Nanotubes. *Chem. Commun.* **2003**, 1442-1443.

(S3) Stadelmann, P. A. EMS - A Software Package for Electron-Diffraction Analysis and HREM Image Simulation in Materials Science. *Ultramicroscopy* **1987**, *21*, 131-145.

(S4) Kociak, M.; Hirahara, K.; Suenaga, K.; Iijima, S. How Accurate Can the Determination of Chiral Indices of Carbon Nanotubes Be? An Experimental Investigation of Chiral Indices Determination on DWNT by Electron Diffraction. *Eur. Phys. J. B* **2003**, *32*, 457-469.

(S5) Lambin, P.; Lucas, A. A. Quantitative Theory of Diffraction by Carbon Nanotubes. *Phys. Rev. B* **1997**, *56*, 3571-3574

(S6) Kirkland, E. *Advanced Computing in Electron Microscopy*; Springer, 2009.

(S7) Peng, L. M.; Ren, G.; Dudarev, S. L.; Whelan, M. J. Robust Parameterization of Elastic and Absorptive Electron Atomic Scattering Factors. *Acta. Crystallogr. Sect. A* **1996**, *52*, 257-276.

(S8) Ricolleau, C.; Nelayah, J.; Oikawa, T.; Konno, Y.; Braidy, N.; Wang, G.; Hue, F.; Florea, L.; Pierron-Bohnes, V.; Alloyeau, D. Performances of an 80-200 kV Microscope Employing a Cold-FEG and an Aberration-Corrected Objective Lens. *J. Electron Microsc.* **2012**, *62*, 283-293

(S9) Che, J.; Çağin, T.; Goddard III, W. Generalized Extended Empirical Bond-Order

Dependent Force Fields Including Nonbond Interactions. *Theor. Chem. Acc.* **1999**, *102*, 346-354

(S10) Hashimoto, A.; Suenaga, K.; Urita, K.; Shimada, T.; Sugai, T.; Bandow, S.; Shinohara, H.; Iijima, S. Atomic Correlation Between Adjacent Graphene Layers in Double-Wall Carbon Nanotubes. *Phys. Rev. Lett.* **2005**, *94*, 045504-4.

(S11) Loiseau, A.; Launois, P.; Petit, S.; Roche, S.; Salvetat, J.-P. *Understanding Carbon Nanotubes, From Basics to Applications*; Springer-Verlag, 2006.

(S12) Liu, K.; Jin, C.; Hong, X.; Kim, J.; Zettl, A.; Wang, E.; Wang, F. Van der Waals-Coupled Electronic States in Incommensurate Double-Walled Carbon Nanotubes. *Nat. Phys.* **2014**, *10*, 737-742.

(S13) Hirahara, K.; Kociak, M.; Bandow, S.; Nakahira, T.; Itoh, K.; Saito, Y.; Iijima, S. Chirality Correlation in Double-Wall Carbon Nanotubes as Studied by Electron Diffraction. *Phys. Rev. B* **2006**, *73*, 195420-11.